Nonlinear $m = 1$ Mode and Fast Reconnection in Collisional Plasmas

A. Y. Aydemir
Institute for Fusion Studies, The University of Texas at Austin, Austin, Texas 78712
(Received 16 August 1996)

Time evolution of the $m = 1$ resistive kink mode is shown to be comprised of two exponential growth phases separated by a transition period during which the growth becomes temporarily algebraic. A modified Sweet-Parker model that takes into account some of the changes in the geometry of the core plasma and the growing island is offered to explain the departure from the algebraic growth of the early nonlinear phase. [S0031-9007(97)03248-1]

PACS numbers: 52.30.Jb, 52.35.Py, 52.65.Kj

The $m = 1$ internal kink mode, modified by various nonideal effects that allow for changes in the magnetic field topology, not only provides a generic mechanism for fast reconnection in laboratory and astrophysical plasmas, but also plays a crucial role in tokamak sawtooth oscillations and high-β disruptions. The goal of this work is to carefully reexamine the nonlinear phase of the resistive $m = 1$ mode and challenge and extend some of the previous work on the subject. Our main conclusion will be that the $m = 1$ mode, when the associated ideal internal kink is at or above marginal stability, grows exponentially until reconnection is complete, thus providing a fast reconnection mechanism even in collisional plasmas. That it can do so in the semicollisional and collisionless regimes was shown in earlier works [1–4]. An extensive discussion of the linear theory of the $m = 1$ mode in various collisionality regimes can be found in the review article by Migliuolo [5].

Interest in the resistive $m = 1$ in the fusion community started with Kadomtsev's proposal [6] that its nonlinear evolution may proceed fast enough to completely reconnect the helical flux within the $q = 1$ rational surface in a characteristic time of $\tau_{\rm rec} = (\tau_{Hp}\tau_R)^{1/2} \sim \eta^{-1/2}$, where $\tau_{Hp} = a/u_{Hp}$, $\tau_R = \mu_0 a^2/\eta_0$, and $u_{Hp} = B_{\rm po}^2/\sqrt{\rho_0\mu_0}$. Here τ_{Hp} and τ_R are the poloidal Alfvén time and the resistive diffusion time, respectively, defined in terms of the minor radius a, a characteristic poloidal field strength $B_{\rm po}$, and resistivity η_0. Subsequent numerical calculations confirmed the basic features of Kadomtsev's conjecture [7,8], and, in fact, suggested that the resistive kink may continue to grow nearly exponentially well into the nonlinear phase. An analytic theory of the nonlinear $m = 1$ island seemed to confirm these expectations of exponential growth [9]. More recently, however, a careful nonlinear analysis [10] and a subsequent numerical calculation [11] seemed to find a transition to an algebraic growth early in the nonlinear development of the mode. Our calculations show that this algebraic growth is only a temporary phase that separates two distinct periods of exponential growth, and that the resistive $m = 1$, although it lacks the explosive nature [1] of the semicollisional and collisionless $m = 1$, does grow exponentially until full reconnection.

Early numerical calculations of the resistive $m = 1$ with modest resolution and at relatively small values of the magnetic Reynolds number $S = \tau_R/\tau_{Hp}$, although not unequivocal, certainly do give an impression of a mode that grows exponentially well into the nonlinear regime [7]; the kinetic energy in the system, a global measure of the mode's time evolution that will be used throughout this paper, grows exponentially before gradually slowing down and saturating. A typical calculation exhibiting this general behavior is shown in Fig. 1(a), where we used $\eta \equiv 1/S = 10^{-5}$. The low-$\beta$ equilibrium used throughout this paper is parametrized by the following safety-factor profile: $q(r) = q_0\{1 + r^{2\lambda}[(q_a/q_0)^{\lambda} - 1]\}^{1/\lambda}$. For Fig. 1(a), we had $q_0 = 0.9$, $q_a = 3$, and $\lambda = 2$. Here a single exponential growth period in the linear phase of the mode gradually blends into the nonlinear regime where the mode slows down for $t \gtrsim 250$, with the growth terminating after complete reconnection around $t \simeq 400$.

The numerical model used here is based on the low-β reduced MHD equations, given in terms of the vorticity U,

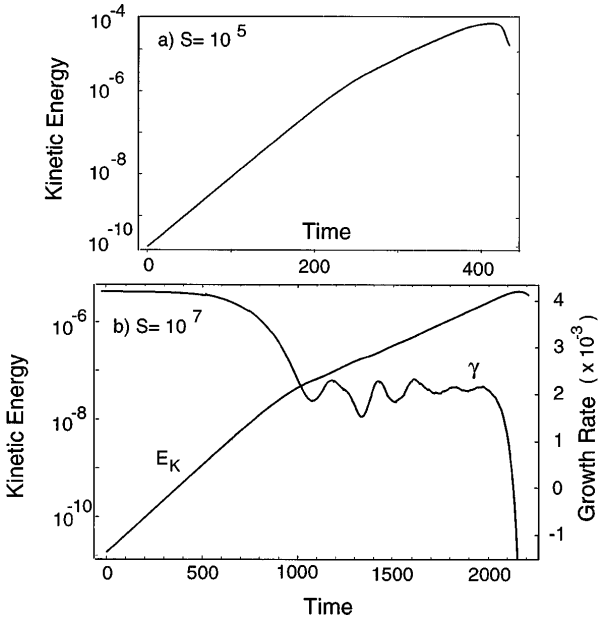

FIG. 1. Results from the nonlinear resistive MHD calculations: (a) The kinetic energy in the mode for $S = 10^5$. (b) The energy and the growth rate for $S = 10^7$.

 0031-9007/97/78(23)/4406(4)$10.00

and the flux function ψ as

$$\frac{\partial U}{\partial t} + [\phi, U] + \nabla_{\parallel} J = \mu \nabla_{\perp}^2 U , \quad (1)$$

$$\frac{\partial \psi}{\partial t} + \nabla_{\parallel} \phi = \eta J , \quad (2)$$

where $J = \nabla_{\perp}^2 \psi$, and $U = \nabla_{\perp}^2 \phi$. The variables have been normalized as follows: $t \to t/\tau_{Hp}, \mathbf{r} \to \mathbf{r}/a$, $\eta = \tau_{Hp}/\tau_R$. The brackets are defined by $[\phi, U] = \hat{\zeta} \cdot \nabla_{\perp} \phi \times \nabla_{\perp} U$, where $\hat{\zeta}$ is a unit vector in the toroidal direction, and $\nabla_{\perp}$ is the 2D gradient in the plane perpendicular to the magnetic field. The parallel gradient operator is defined as $\nabla_{\parallel} J = \partial J/\partial \zeta + [J, \psi]$ for any scalar J.

At higher values of S, the calculations become more challenging because of the well-known nearly singular behavior of the current density in the resistive layer (Fig. 2). Formation of a current sheet here presents a number of difficulties. Computationally, adequate resolution of the current sheet as it deepens and moves outward becomes difficult and requires a mesh that dynamically evolves with it. It is also susceptible to secondary instabilities which tend to break it up, affecting the nonlinear behavior of the original mode in a rather complicated fashion [12]. While the instability of the current sheet cannot always be avoided, it is possible to deal successfully with the computational challenge of resolving the layer at all times. Such a calculation is shown in Fig. 1(b), where we repeat the calculation of Fig. 1(a) at $S = 10^7$. The most significant feature of this figure is the appearance of two distinct exponential growth phases, separated by a relatively short transition period. The first one ($t \lesssim 800$), of course, represents the linear phase of the mode, where the island width is less than the resistive layer width, $W \lesssim \delta_l = (\eta/k_{\parallel}')^{1/3}$. As the island becomes nonlinear ($W \gtrsim \delta_l$), the mode slows down, as was also seen for $S = 10^5$. However, whereas in Fig. 1(a) the time scale for the nonlinear period was not long enough (before complete reconnection occurred) to discern a second exponential phase, Fig. 1(b) clearly shows, for $1200 \lesssim t \lesssim 2000$, a nonlinearly exponentiating mode before the growth terminates with complete reconnection. The growth rate of the mode shown as a function of time in Fig. 1(b) displays this transition from linear to the nonlinear phase, with the nonlinear growth rate being approximately half of the linear one, $\gamma_{\text{non}} \simeq \gamma_l/2$. Oscillations in $\gamma(t)$ in the nonlinear phase of Fig. 1(b) represent the ringing that is commonly observed during "phase transitions" in nonlinear calculations; they become less pronounced with increased viscous dissipation, which was kept to a minimum here.

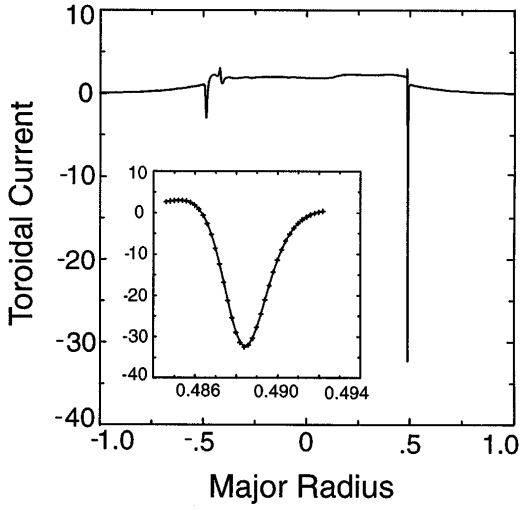

FIG. 2. The toroidal current and a magnified view of the current sheet.

It is difficult to offer a rigorous theory of reconnection that would be valid in the deeply nonlinear regime of the $m = 1$ mode; however, a simple modification of the Sweet-Parker argument that takes into account some of the changes in the geometry at late stages of the island evolution seems to capture the essential features of the fully nonlinear calculation presented earlier. This modified Sweet-Parker argument is presented below.

Assuming a rigid shift of the core plasma and helicity conservation during reconnection [6,10], the island evolution can be presented as in Fig. 3(a). Figure 3(b) shows how the helical flux $\psi^* = \psi + r^2/2$ changes during this process [see also Fig. 3 of Ref. [11]]. Here, the helical flux is related to the auxiliary field B_θ^* and the equilibrium safety factor profile $q(r)$ through $B_\theta^* = -\partial \psi^*/\partial r = r[1/q(r) - 1]$. The point O denotes the location of the original magnetic axis; the point O', radially displaced from O by an amount $\xi(t)$, is its location at some time t, giving an island width of $W(t) \simeq 2\xi$. The radius of the core plasma at this time is given by $r_c(t)$, as measured from O'. The radius of the outer separatrix of the island, as measured from the point O, is given by $r_s(t)$. The initial values for these quantities are $\xi(0) = 0$, and $r_c(0) = r_s(0) = r_{s0}$, where r_{s0} is the radius of the $q = 1$ surface in the equilibrium state. The outer separatrix radius $r_s(t)$ is implicitly determined by $\psi^*(r_s(t) - \xi(t)) = \psi^*(r_s(t))$, which follows from the rigid shift and helicity conservation assumptions [see Fig. 3(b)].

Mass conservation in the reconnection layer with an incompressible flow leads to the usual relation $u_r \sim (\delta/L) u_\theta$, where u_r is the inflow velocity at the

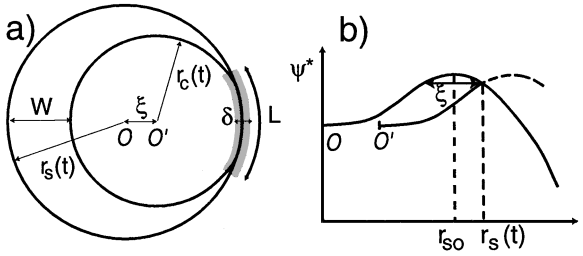

FIG. 3. (a) The $m = 1$ island geometry used in the modified Sweet-Parker model. (b) Evolution of the helical flux during reconnection.

midplane, and u_θ is the outflow velocity. The lengths δ and L measure the layer's radial width and its poloidal extent, respectively. Recognizing the lack of rigor in this Sweet-Parker argument, we simply identify the inflow velocity with the rate of displacement of the core plasma, and the outflow velocity with the upstream Alfvén speed and use $u_r = d\xi/dt$, $u_\theta \simeq B_\theta^*(r_s(t) - \xi(t))$.

The layer length L is obviously proportional to the core plasma radius. Analyses of the early nonlinear phase have typically assumed $L \simeq r_{s0}$ [11,13]. However, in the deep nonlinear phase, shrinking core plasma radius leads to a corresponding decrease in the length L. This effect competes with the narrowing of the layer in determining the reconnection rate and will be seen below to account for the termination of the algebraic growth and reestablishment of a new "exponential phase." In earlier works, a decrease in L was shown to lead to an explosive growth in the semicollisional/collisionless regime [1–4]; however, there the reconnection layer physics and the accompanying change from a "Y point" to an "X point" geometry were the mechanisms responsible for the decrease, not the intrinsic geometric changes in the shrinking core plasma that is being considered here. These two separate effects are obviously additive in the semicollisional/collisionless case, but the former does not exist in the collisional plasmas considered here.

Assuming that the flux surfaces remain circular in the core and ignoring multiplicative factors of order unity, the layer length will be taken to be $L(t) \equiv r_c(t) = r_s(t) - \xi(t)$. For small $\xi \ll r_{s0}$, this assumption leads to $L \sim r_{s0} - \xi/2$, indicating that L decreases at half the core displacement rate in the early nonlinear phase. The layer width δ is related to the inflow velocity through the parallel Ohm's law. Whereas all three terms of the Ohm's law in Eq. (2) are comparable within the resistive layer in the linear regime, the convective and diffusive terms become dominant in the nonlinear reconnection layer. Writing them in terms of the helical flux ψ^* and using $u_r B_\theta^*(r_s(t) - \xi) \sim \eta[B_\theta^*]/\delta$, we get $\delta(t) = \eta\{B_\theta^*(r_s(t))/B_\theta^*(r_s(t) - \xi) + 1\}/(d\xi/dt)$, where $B_\theta^*(r_s(t) - \xi)$ and $B_\theta^*(r_s(t))$ represent the auxiliary field amplitudes on two sides of the neutral line at $r = r_s(t)$ in Fig. 3(b). Substituting for δ, L, and u_θ in the mass continuity equation finally leads to an equation governing the nonlinear evolution of the core plasma displacement

$$\left(\frac{d\xi}{dt}\right)^2 = \alpha\,\frac{\eta}{L(t)}\{B_\theta^*(r_s(t) + \Delta) + B_\theta^*(r_s(t) - \xi(t) - \Delta)\}. \tag{3}$$

The extra degrees of freedom introduced by the constants α and Δ are needed to satisfy the continuity constraints on $d\xi/dt$ and $d^2\xi/dt^2$ that will be discussed below.

The displacement in the linear regime is simply determined by

$$\frac{d\xi}{dt} = \gamma_l \xi\,, \tag{4}$$

where $\gamma_l = k_\parallel'^{2/3}\eta^{1/3}$ is the linear growth rate. This exponential phase is valid for $\xi < \delta_l$ whereas Eq. (3) becomes applicable for $\xi > \delta_l$. However, there is a short period corresponding to $\xi \simeq \delta_l$ not described by the linear physics giving rise to Eq. (4), or the nonlinear physics leading to Eq. (3). Ignoring this late linear (or very early nonlinear) phase of the mode here, the exponentially growing linear phase [Eq. (4)] will be directly connected to the nonlinear phase described by Eq. (3) using continuity of $d\xi/dt$, and $d^2\xi/dt^2$ at some point $t = t_0$, $\xi(t_0) = \xi_0 \equiv c\,\delta_l \ll r_{s0}$, where $c \sim \mathcal{O}(1)$ is some constant to be chosen later. Thus, using Eq. (4) for $t \le t_0$ and Eq. (3) for $t > t_0$, and letting $r_s(t) \simeq r_{s0} + \xi/2$ for $\xi \ll r_{s0}$, the continuity constraints can be shown to give $\alpha = 2c\{1 + \mathcal{O}(\xi_0/r_{s0})\}$, and $\Delta = -\xi_0/4\{1 + \mathcal{O}(\xi_0/r_{s0})\}$ in Eq. (3).

In general, Eq. (3) can be solved only numerically; but for $\xi \ll r_{s0}$, expanding B_θ^* around $r = r_{s0}$, we obtain a simpler version

$$\left(\frac{d\xi}{dt}\right)^2 = \frac{2c\,\eta\, r_{s0} k_\parallel'}{L(t)}\left(\xi - \frac{\xi_0}{2}\right), \tag{5}$$

where we used $B_\theta^{*\prime}(r_{s0}) = r_{s0}k_\parallel'(r_{s0})$. For $L(t) \simeq r_{s0}$, Eq. (5) has an algebraic solution [11], valid in the early nonlinear phase of the mode: $\xi(t) = \xi_0/2 + [(\xi_0/2)^{1/2} + (c\,\eta k_\parallel'/2)^{1/2}(t - t_0)]^2$ for $t \ge t_0$. However, as the displacement grows in time, this algebraic behavior is modified when $\xi \gg \xi_0$, and both Eqs. (3) and (5) predict a new exponential phase. General solutions of Eqs. (3) and (4) are shown in Fig. 4 for various parameters and compared with results from the nonlinear resistive MHD calculations. Here the initial condition and the growth rate for Eq. (4) are chosen to match the linear phase of the nonlinear MHD calculation. Thus, the only free parameter in the system is the constant c, which determines the location of the beginning of the nonlinear phase in the model equations. Figure 4(a) shows solutions to Eqs. (3) and (4) for three different values of this parameter. Evidently, $c = 1$, corresponding to $t_0 = 431$, $\xi_0 = \delta_l$, does not provide a very good match to the result from the nonlinear MHD calculation shown by the solid line. The case with $c = 3$ ($t_0 = 694$, $\xi_0 = 3\delta_l$), however, agrees quite well, not only with the position of the knee in the kinetic energy but also with the subsequent nonlinear development of the mode, as seen in Fig. 4(a). Figure 4(b) compares the inflow velocity $d\xi/dt$ obtained from Eqs. (3) and (4) for $c = 3$ using $L = r_s(t) - \xi(t)$ (the solid line), and $L = r_{s0}$ (the dashed line). As expected, with the constant layer length $L = r_{s0}$, the velocity grows only algebraically ($u_r \sim t$) in the nonlinear regime, whereas the variable length solution gradually departs from this algebraic behavior and becomes "exponential" for $\xi \gg \xi_0 = 3\delta_l$.

Obviously, the time evolution predicted by this simple model is not purely exponential in the nonlinear regime. In fact, it terminates with a finite-time singularity when $L(t) = r_s(t) - \xi \to 0$. This singularity, however, is not

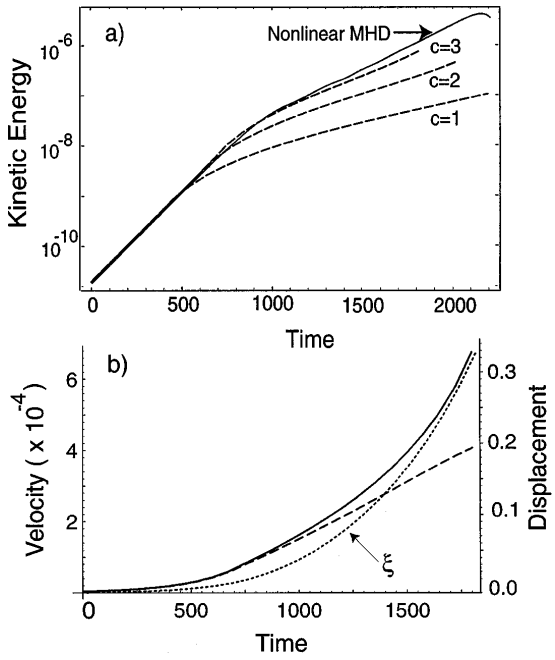

FIG. 4. (a) The solid line: the nonlinear MHD result. The dashed lines: the modified Sweet-Parker model for three different values of the parameter $c = \xi_0/\delta_l$. (b) The inflow velocity predicted by the model. The dashed line: Lr_{s0} (constant), the solid line: $L = r_s(t) - \xi(t)$. Also shown is the time history of the displacement for this second case (dotted line).

physical and points to a failure of the modified Sweet-Parker model towards the end of reconnection when the displacement is of the order of the mixing radius. A more complete model would have to take into account, among other factors, diminishing of the instability drive as the flux in the core is exhausted through reconnection, and the elliptical deformation of the core flux surfaces and a more physical estimate of the reconnection layer length for large ξ. These corrections are left for future work. With these shortcomings in mind, one can nevertheless obtain a quantitative estimate for the nonlinear growth rate predicted by this modified Sweet-Parker model, starting with Eq. (5). Defining a nonlinear growth rate by $\gamma_{\rm non} \equiv \mathrm{Min}\{(d^2\xi/dt^2)/(d\xi/dt)\}$ leads to

$$\frac{\gamma_{\rm non}}{\gamma_l} = \frac{8\sqrt{c}}{3\sqrt{3}}\left\{\frac{\delta_l}{r_{s0}}\right\}^{1/2}. \qquad (6)$$

The minimum occurs at $\xi = r_{s0}/2$. Using the parameters of the nonlinear MHD calculation shown in Fig. 1(b) gives $\gamma_{\rm non}/\gamma_l \simeq 0.31$ for $c = 3$, which is somewhat lower than the average growth rate obtained from the MHD calculation, $\gamma_{\rm non}/\gamma_l \simeq 0.5$. However, the average nonlinear growth rate of the model is closer to that of the nonlinear MHD calculation, as seen in Fig. 4(a). Note that $(\gamma_{\rm non}/\gamma_l) \sim \eta^{1/6}$, indicating a very weak dependence on resistivity.

In summary, in the first part of the paper, careful numerical calculations show that the resistive $m = 1$ mode does indeed grow exponentially until full reconnection. The initial linear phase, where the mode grows at the linear growth rate, is separated from the nonlinear phase by a transition period during which the growth becomes algebraic. In the deeply nonlinear phase, the growth is again exponential; this second period persists until all the flux within the original $q = 1$ surface is reconnected. This continued exponential growth, albeit at a reduced rate in the nonlinear regime, implies a faster reconnection time for the resistive $m = 1$ than the simple Sweet-Parker scaling of Kadomtsev. Thus, even without invoking semicollisional or collisionless physics [1–4] that is valid in high temperature plasmas, the $m = 1$ mode may provide an adequate explanation for fast magnetic reconnection and rapid sawtooth crash times, especially in the more collisional regime. In the second part of the paper, the conventional Sweet-Parker argument is modified to take into account some of the geometric changes in the core plasma, such as the shortening of the reconnection layer with decreasing core radius, to show that the algebraic phase is only temporary. Decreasing layer length competes with the narrowing of the reconnection layer width and leads to a new exponential phase in agreement with the nonlinear MHD calculations presented earlier. The geometric changes considered here are independent of the linear layer physics and are expected to contribute strongly to the nonlinear evolution of the semicollisional and collisionless modes also.

This work was supported by the U.S. Department of Energy under Grant No. DE-FG03-96ER-54346.

[1] A. Y. Aydemir, Phys. Fluids B **4**, 3469 (1992).
[2] X. Wang and A. Bhattacharjee, Phys. Rev. Lett. **70**, 1627 (1993).
[3] M. Ottaviani and F. Porcelli, Phys. Rev. Lett. **71**, 3802 (1993).
[4] B. Rogers and L. Zakharov, Phys. Plasmas **3**, 2411 (1996).
[5] S. Migliuolo, Nucl. Fusion **33**, 1721 (1993).
[6] B. B. Kadomtsev, Fiz. Plazmy **1**, 710 (1975) [Sov. J. Plasma Phys. **1**, 389 (1975).
[7] B. V. Waddell, M. N. Rosenbluth, D. A. Monticello, and R. B. White, Nucl. Fusion **16**, 3 (1976).
[8] A. Sykes and J. A. Wesson, Phys. Rev. Lett. **37**, 140 (1976).
[9] R. D. Hazeltine, J. D. Meiss, and P. J. Morrison, Phys. Fluids **29**, 1633 (1986).
[10] F. L. Waelbroeck, Phys. Fluids B **1**, 2372 (1989).
[11] Dieter Biskamp, Phys. Fluids B **3**, 3353 (1991).
[12] Dieter Biskamp, Phys. Fluids **29**, 1520 (1986).
[13] L. Zakharov, B. Rogers, and S. Migliuolo, Phys. Fluids B **5**, 2498 (1993).